while the tetrachloro complex is no longer a probable candidate for the 410-nm transient, the aquated forms to varying degrees are realistic possibilities, including possibly cases such as $[PtCl(OH)_3]^-$ that have not been considered here. In general, then, the possibility exists, on the basis of these model studies, that the 410-nm band may not always be indicative of a single species or even the same one under different conditions, and in the following paper, we present the experimental results and compare them to those obtained here by the use of the Xα method.

Acknowledgment. These calculations have been performed at the CNUSC (Montpellier, France) and the CC-IN2P3 (Lyon, France). The financial support provided by the Natural Sciences and Engineering Research Council of Canada to W.L.W. and by the North Atlantic Treaty Organization (Project No. 0680/85) is very much appreciated.

Contribution from the Department of Chemistry and the Saskatchewan Accelerator Laboratory, University of Saskatchewan, Saskatoon, Saskatchewan S7N 0W0, Canada, Bereich Strahlenchemie, Hahn-Meitner-Institut, Postfach 39 01 28, D-1000 Berlin 39, Ecole de Chimie, 34075 Montpellier Cedex, France, and Institut de Physique Nucléaire (et IN2P3), Université de Lyon I, 68622 Villeurbanne Cedex, France

Photolytic and Radiolytic Study of Platinum(III) Complex Ions Containing Aquo and Chloro Ligands

W. L. Waltz,*[1a] J. Lilie,[1b] A. Goursot,[1c] and H. Chermette[1d]

Received July 22, 1988

The formations and characterizations of short-lived, monomeric platinum(III) complex ions containing aquo and chloro ligands have been studied by using pulse radiolysis and laser photolysis techniques coupled with UV–visible absorption and conductivity detection methods. Five different chemical routes have been used to generate in aqueous media the same or similar platinum(III) species: reaction of tetrachloroplatinum(II), $[PtCl_4]^{2-}$, with the hydroxyl radical, interactions of hexachloroplatinum(IV), $[PtCl_6]^{2-}$, with the hydrated electron, hydrogen atom, and *tert*-butyl alcohol radical, and the 265-nm photolysis of $[PtCl_6]^{2-}$ with the latter giving rise to both oxidation–reduction and ligand-substitution processes. The platinum(III) intermediates can be classified into two categories. The nascent or shorter lived species exhibit intense charge-transfer bands with peak maxima near 450 nm or at wavelengths below 300 nm, and they are proposed to be of a distorted-octahedral type with compositions of the form $[Pt^{III}(Cl)_{6-m}(X)_m]$ (m = 0–2; X = OH, H_2O). The longer lived Pt(III) complexes are characterized by a single charge-transfer band having a peak between 410 and 420 nm and by compositions of the type $[Pt^{III}(Cl)_{4-n}(X)_n]$ (n = 1–3; X = OH, H_2O) having limiting square-planar structures. The mechanisms for the formations of the platinum(III) complex ions and for their interrelationships are discussed, and evidence is presented to indicate that these species act as catalytic agents in the thermal aquation of $[PtCl_6]^{2-}$.

Introduction

A number of experimental investigations using fast reaction techniques coupled with UV–visible absorption detection have established that the radiolytic and photolytic reactions in aqueous media of octahedral hexachloroplatinum(IV) ion, $[PtCl_6]^{2-}$, and of the square-planar tetrachloroplatinum(II) complex, $[PtCl_4]^{2-}$, can give rise to transitory species characterized as monomeric platinum entities in which the metal center is in the unusual formal oxidation state of +3.[2-8] The reaction of the hydroxyl radical and $[PtCl_4]^{2-}$ yields as the nascently observed product a species with an absorption maximum near 450 nm that subsequently decays via a first-order rate law to generate a longer lived transient having a peak near 410 nm.[2,3] While earlier workers recognized the possibility that the initial process could involve an electron-transfer mechanism, they proposed that the process is one incorporating OH addition to the metal center to give the five-coordinate, square-pyramidal product $[PtCl_4(OH)]^{2-}$. Its subsequent intramolecular rearrangement to a trigonal-bipyramidal form is then associated with the absorption peak at 410 nm. The nascent absorption at 450 nm was, however, not observed at low or high pHs: in alkaline media, the indications were that both the initial and longer lived intermediates now exhibited peaks near 390 nm. No detailed explanations were offered to account for these acid–base effects even though they appear to be at variance with the proposed intramolecular mechanism.

The same or similar species absorbing at 410 nm (but none exhibiting a peak at 450 nm) have been observed in the reaction of the hydrated electron, e_{aq}^-, and $[PtCl_6]^{2-}$ and in the conventional flash photolysis of $[PtCl_6]^{2-}$.[2,4] More recent results, obtained by picosecond laser photolysis and interpreted with aid of theoretical calculations performed by using multiple-scattering MO Xα theory, clearly point to the initial photoredox product as being the short-lived, square-pyramidal $[PtCl_5]^{2-}$.[7] While here it was not feasible experimentally to determine the nature of the subsequent product(s) arising from the rapid decay of $[PtCl_5]^{2-}$ (τ = 210 ps), the probable implication would be that such could be the longer lived species (micro- to millisecond scales) absorbing at 450 and 410 nm.

A key observation in regard to the 410-nm transient and one that is consistent with its designation as a platinum(III) complex ion is its reaction with $Fe^{2+}(aq)$.[4] From the influence of ionic strength on this process, Wright and Laurence concluded that its overall electrostatic charge was −1. As this feature is not consistent with the charge of −2 for the species proposed by Adams and co-workers,[2] the former authors suggested that the 410-nm intermediate was $[PtCl_4]^-$, having a square-planar form with possibly two labile apical positions.[4] However, the validity of the overall charge measurement has been questioned.[6]

While these earlier studies have brought to light a number of intriguing features about platinum(III) chloro complexes, no consistent picture has yet emerged as to their compositions/structures or to their mechanistic interrelationships. Furthermore, the results of theoretical calculations do not in general support the 410- and 450-nm transients as being five-coordinate.[9-11] In

* To whom correspondence should be addressed.

(1) (a) University of Saskatchewan. (b) Hahn-Meitner-Institut. (c) Ecole de Chimie. (d) Université de Lyon I.
(2) Adams, G. B.; Broskiewicz, R. B.; Michael, B. D. *J. Chem. Soc., Faraday Trans. 1* **1968**, *64*, 1256–1264.
(3) Ghosh-Mazumdar, A. S.; Hart, E. J. *Int. J. Radiat. Phys. Chem.* **1969**, *1*, 165–176.
(4) Wright, R.; Laurence, G. S. *J. Chem. Soc., Chem. Commun.* **1972**, 132–133.
(5) Storer, D. K.; Waltz, W. L.; Brodovitch, J. C.; Eager, R. L. *Int. J. Radiat. Phys. Chem.* **1975**, *7*, 693–704.
(6) Broszkeiwicz, R. K.; Grodkowski, J. *Int. J. Radiat. Phys. Chem.* **1976**, *8*, 359–365.
(7) Goursot, A.; Kirk, A. D.; Waltz, W. L.; Porter, G. B.; Sharma, D. K. *Inorg. Chem.* **1987**, *26*, 14–18.
(8) Anbar, M.; Bamenek, M.; Ross, A. B. *Natl. Stand. Ref. Data Ser. (U.S., Natl. Bur. Stand.)* **1973**, *NSRDS-NBS43*.

0020-1669/89/1328-2247$01.50/0

a related context, investigations into the generation and characterization of monomeric platinum(III) amine complex ions have led to emphasis being placed on the initial products being of a distorted-octahedral type incorporating aquo and hydroxo ligands (rather than five-coordinate species) in order to account for the presence of acid–base effects.[12,13]

The underlying objective of the current investiation has been to attain an enlarged and more detailed understanding into the natures of platinum(III) chloro species and their interrelationships through the use of more comprehensive approaches. In the preceding article,[11] we have presented the results of the application of MS Xα MO theory as a means to calculate charge-transfer (CT) absorption spectra for comparison to experimental spectra and, in so doing, to obtain clearer insight into the possible structural forms associated with platinum(III) chloro complex ions. In this paper, the findings obtained from pulse radiolysis and laser photolysis experiments are given, and a salient aspect has been the combined use of optical absorption and conductivity detection techniques. The latter has been particularly effective in discerning the presence or absence of charge-transfer phenomena. For example, the conductivity results for the reaction of OH and $[PtCl_4]^{2-}$ confirm the earlier suggestion by Adams and co-workers[2] that the nascent process is indeed one of oxidative addition rather than an electron-transfer process; however, these findings also show that the subsequent interconversion of the 450-nm product to that of the 410-nm one is not simply an intramolecular rearrangement but that it involves incorporation of a hydroxide ligand. By use of the aforementioned methods and increased time resolution (relative to those of the earlier studies), it has proven feasible to define more succinctly the mechanistic events associated with the photochemistry of $[PtCl_6]^{2-}$ and with this complex's reaction with e_{aq}^- and also to discover new routes to the formation of platinum(III) intermediates involving the reactions of $[PtCl_6]^{2-}$ with the H atom and with the *tert*-butyl alcohol radical. Evidence is presented that establishes a more direct link between the occurrence of Pt(III) intermediates and their putative roles as catalytic agents in thermal or steady-state photolytic processes associated with ligand exchange or substitution.[14,15]

Experimental Section

Apparatus, Actinometry, and Dosimetry. The pulse radiolysis and flash-laser photolysis systems and their associated conductivity and UV–visible absorption detection equipment have been described elsewhere.[12,16] Of general note is that the transient phenomena discussed in this work represent the difference between the signal for the irradiated solution and that for the unirradiated one, recorded at room temperatures (20–28 °C), and such changes have been calibrated against the behaviors of standard solutions. For photolysis at 265 nm, a frequency-quadrupled Q-switched neodymium-yag laser was used with the actinometry being based upon the photoproduction of e_{aq}^- from potassium ferrocyanide solutions.[17] The dosimetry for both conductivity and optical measurements was performed with potassium bromide or tetranitromethane reference media,[18–20] and the following G values (number of a given species formed per 100 eV of energy absorbed) have been taken for the primary aqueous species: $G_{e^-} = G_{H^+} = 2.7$, $G_{OH} = 2.8$, $G_H = 0.55$.[8,21] The values employed for the equivalent ionic conductivities of the proton, hydroxide ion, and electron were 350, 197, and 190 Ω^{-1} cm^2, respectively, and those for the anionic platinum complexes have been taken as 70 Ω^{-1} cm^2.[8,22,23] Numbers in parentheses refer to the number of independent measurements, and the precision errors are given as estimated standard deviations.

Materials and Solutions. Potassium tetrachloroplatinate(II), $K_2[PtCl_4]$ (Johnson Matthey-ASEAR, 99.9%), and potassium hexachloroplatinate(IV), $K_2[PtCl_6]$ (Morton Thiokol-Alfa Products, 99.9%), were used as received. Since these substances, in particular $[PtCl_4]^{2-}$,[24] will undergo aquation, studies on their solutions were in general carried out within 1–3 h of their preparation, and over these periods of time, reproducible results were obtained. In the investigation of the reaction of the hydroxyl radical and $[PtCl_4]^{2-}$ in basic media (pH ca. 11), we observed that the optical spectrum and kinetic results for a solution that had been aged for 22 h differed somewhat from those obtained for fresh solutions (see Results and Discussion); however, the former were in closer agreement to those reported by others.[3] This suggests in this instance that the slight numerical differences between our values and earlier ones may reflect to some degree differences in the extent of aquation.

Other materials used in the present study were of reagent quality. Deaeration of solutions, prepared from water obtained from a Millipore Super-Q system, was carried out by bubbling with argon or purified nitrous oxide: the latter gas was also employed to convert the hydrated electron into hydroxyl radical.[21] Changes in the alkalinity or acidity of the media were made through addition of sodium hydroxide or perchloric acid, and sodium perchlorate was added where needed to adjust the ionic strength of the solutions.

Results and Discussion

Pulse irradiation of dilute aqueous solutions by high-energy electrons (ca. 10 MeV) as used in this work leads to the generation of aqueous free radicals, hydrogen ion, and small amounts of H_2 and H_2O_2 (eq 1); however, the molecular products are not gen-

$$H_2O \overset{e^-}{\rightsquigarrow} e_{aq}^-,\ H,\ OH,\ H^+,\ H_2,\ H_2O_2 \qquad (1)$$

erally reactive on pulse radiolysis time scales (nanoseconds to milliseconds). By contrast, the radical species are highly reactive toward platinum complexes and between like and unlike radicals.[8,21,25] To minimize the occurrence of the latter reactions, low radical concentrations (<ca. 3 μM) have been used, and the levels of the platinum complex ions are in considerable excess over those of the aqueous radicals so that, in their reactions with the platinum materials, pseudo-first-order conditions will prevail. In addition, standard scavenging procedures such as those shown below have been employed.[8,21,25,26] The reactions of eq 2 and 3

$$e_{aq}^- + H^+ \rightarrow H \qquad (2)$$

$$e_{aq}^- + N_2O \xrightarrow{H^+} N_2 + OH \qquad (3)$$

$$OH + (CH_3)_3COH \rightarrow H_2O + {}^\bullet CH_2C(CH_3)_2OH \qquad (4)$$

$$H + O_2 \rightarrow HO_2 \qquad (5)$$

exemplify the interconversion of one primary radical into another, which is useful in reducing the complexity of the situation due to the initial presence in deaerated media of three different types of aqueous radicals. The processes of eq 4 and 5 illustrate the conversion of reactive aqueous radicals into less reactive species. Since the reactants and products of eq 4 and 5 do not absorb significantly at wavelengths beyond about 300 nm whereas the platinum(III) entities do exhibit intense CT bands in the visible region, the effects of the presence of oxygen or *tert*-butyl alcohol on the formation of Pt(III) intermediates serve as diagnostic tests for the participation of OH or H. Through the judicious choice of conditions, it has been feasible to maximize the presence of a

(9) Goursot, A.; Chermette, H.; Penigault, E.; Chanon, M.; Waltz, W. L. *Inorg. Chem.* **1984**, *23*, 3618–3625.
(10) Goursot, A.; Chermette, H.; Chanon, M.; Waltz, W. L. *Inorg. Chem.* **1985**, *24*, 1042–1047.
(11) Goursot, A.; Chermette, H.; Waltz, W. L.; Lilie, J. *Inorg. Chem.*, preceding paper in this issue.
(12) Waltz, W. L.; Lilie, J.; Walters, R. T.; Woods, R. J. *Inorg. Chem.* **1980**, *19*, 3284–3291.
(13) Khan, H. M.; Waltz, W. L.; Lilie, J.; Woods, R. J. *Inorg. Chem.* **1982**, *21*, 1489–1497.
(14) Rich, R. L.; Taube, H. *J. Am. Chem. Soc.* **1954**, *76*, 2608–2611.
(15) Cox, L. E.; Peters, D. G.; Wehry, E. L. *J. Inorg. Nucl. Chem.* **1972**, *34*, 297–305.
(16) Waltz, W. L.; Lilie, J.; Lee, S. H. *Inorg. Chem.* **1984**, *23*, 1768–1775.
(17) Shiron, M.; Stein, G. *J. Chem. Phys.* **1971**, *55*, 3372–3378.
(18) Asmus, K.-D. *Int. J. Radiat. Phys. Chem.* **1972**, *4*, 417–437.
(19) Chaudhri, S. A.; Asmus, K.-D. *J. Chem. Soc., Faraday Trans. 1* **1972**, *68*, 385–392.
(20) Henglein, A.; Lindig, B.; Westerhausen, J. *Radiat. Phys. Chem.* **1984**, *23*, 199–205.
(21) Dorfman, L. M.; Adams, G. B. *Natl. Stand. Ref. Data Ser. (U.S., Natl. Bur. Stand.)* **1973**, *NSRDS-NBS46*.
(22) Landolt-Börnstein. *Zahlenwerte und Functionen*, 6th ed.; Springer-Verlag: Berlin, 1960; Vol. II, Part 7, pp 259–260.
(23) Dreyer, R.; Dreyer, I.; Rettig, D. *Z. Phys. Chem. (Leipzig)* **1963**, *224*, 199–206.
(24) Basolo, F.; Pearson, R. G. *Mechanisms of Inorganic Reactions*, 2nd ed.; Wiley: New York, 1967; p 386.
(25) Anbar, M.; Farhataziz; Ross, A. B. *Natl. Stand. Ref. Data Ser. (U.S., Natl. Bur. Stand.)* **1975**, *NSRDS-NBS51*.
(26) Simic, M.; Neta, P.; Hayon, E. *J. Phys. Chem.* **1969**, *73*, 3794–3800.

Table I. Spectral Summary for 450- and 410-nm Species

originating reactants	pH	450-nm band[a] peak, nm	fwhm, nm	$10^{-3}\epsilon$, M^{-1} cm^{-1}	410-nm band[a] peak, nm	fwhm, nm	$10^{-3}\epsilon$, M^{-1} cm^{-1}	$\epsilon_{410}/\epsilon_{450}$	apparent isosbestic pt, nm[a]
OH + $[PtCl_4]^{2-}$ [b]	4.5	455	85	3.5	415	65	4.4	(1.3 ± 0.1)/1	440
	10.7	415	>100	2.9	395	65	4.2	(1.4 ± 0.1)/1	420
	11.1	410	80	3.3	410	60	4.4	(1.3 ± 0.1)/1	430
t-Bu radical + $[PtCl_6]^{2-}$ [c]	4.2				420	65	3.8		
e_{aq}^- + $[PtCl_6]^{2-}$ [d]	5.1	450		ca. 3.4	415	65	4.1[e]	ca. 1.2/1	440
H + $[PtCl_6]^{2-}$ [d]	2.6	455	90	2.2	420	65	3.9[e]	(1.8 ± 0.1)/1	450
	2.2	ca. 445		ca. 1.4	420	50	4.2[e]	ca. 3/1	465
photochem of $[PtCl_6]^{2-}$ [f]	4.5	445	75		410	50		(1.6 ± 0.3)/1	435

[a] Estimated standard deviations: molar absorption coefficient (ϵ), ±10%; wavelength, ±5 nm. fwhm = full width at half-maximum. [b] Conditions: N_2O saturated; 80–290 μM $[PtCl_4]^{2-}$; solution at pH 10.7 aged 22 h. [c] Conditions: N_2O saturated; 200 μM $[PtCl_6]^{2-}$; 0.11 M *tert*-butyl alcohol (*t*-Bu). The 450-nm band was not observed: see text. [d] Conditions: Ar saturated; 100 μM $[PtCl_6]^{2-}$; 0.11 M *tert*-butyl alcohol. [e] Corrected by 18% for absorption by product of the *tert*-butyl alcohol radical reaction. [f] Conditions: Ar saturated; 40 μM $[PtCl_6]^{2-}$. The ratio $\epsilon_{410}/\epsilon_{450}$ is that for absorbances at 410 and 445 nm.

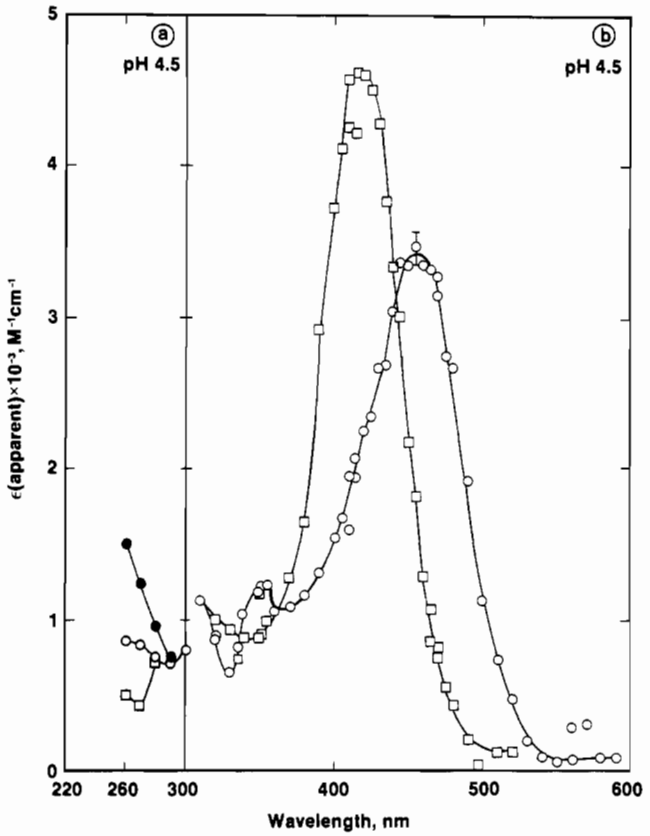

Figure 1. Absorption arising from the reaction of OH and $[PtCl_4]^{2-}$ in solutions saturated with N_2O at pH 4.5: (a) 81 μM $[PtCl_4]^{2-}$ after (○) 3 μs, (●) 3 μs corrected for absorption loss of starting material, and (□) 40 μs; (b) 249 μM $[PtCl_4]^{2-}$ after (○) 1 μs and (□) 40 μs.

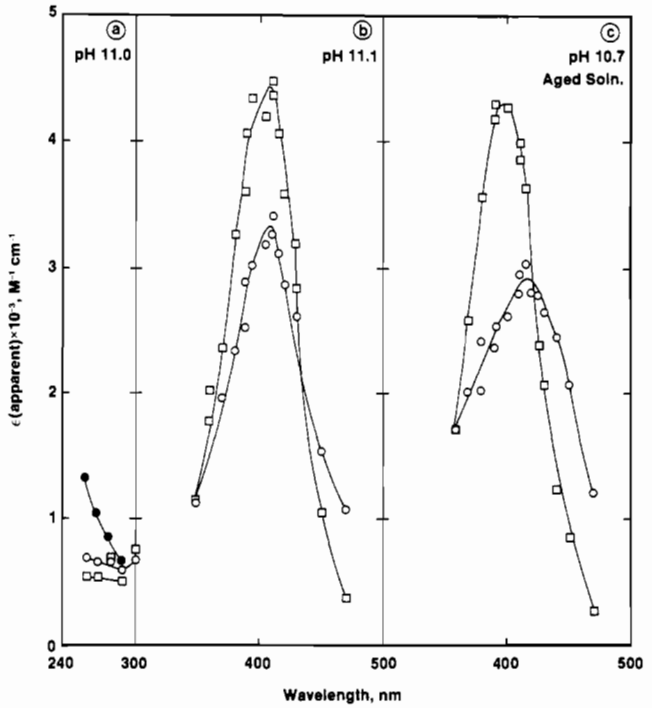

Figure 2. Absorption spectra arising from the reaction of OH and $[PtCl_4]^{2-}$ in basic solutions saturated with N_2O: (a) 85 μM $[PtCl_4]^{2-}$, pH 11.0, after (○) 10 μs, (●) 10 μs corrected for absorption by starting material, and (□) 40 μs; (b) 250 μM $[PtCl_4]^{2-}$, pH 11.1, after (○) 20 μs and (□) 800 μs; (c) 288 μM $[PtCl_4]^{2-}$ aged for 22 h, pH 10.7 (1×10^{-3} M NaOH), after (○) 3 μs and (□) 80 μs.

given radical and in most instances to ensure that it reacts with the platinum substrate to an extent in excess of 90%.

Reactions Associated with OH and $[PtCl_4]^{2-}$. In solutions containing 85–507 μM $[PtCl_4]^{2-}$ and saturated with N_2O, the hydrated electron, e_{aq}^-, will react rapidly ($t_{1/2}$ ca. 4 ns) and almost exclusively with N_2O so that, near the end of the irradiation pulse, the major radical will be OH (ca. 90%).[3,8] The remaining 10% will be H atom, which, although it is reactive toward $[PtCl_4]^{2-}$, does not appear to contribute significantly here to changes in conductivity and absorption: the low-intensity band with a peak near 310 nm (Figure 1) has been ascribed in part to the product of the H atom reaction.[2,3]

As shown in Figures 1 and 2, the major absorption change occurs as an increase in the 350–500-nm region with a smaller increase between 260 and 300 nm and with essentially no movement between 600 and 720 nm. Salient features of the spectra are given in Table I. The addition of *tert*-butyl alcohol (0.11 or 0.57 M), an efficient scavenger for OH but not for the H atom, eliminates the initial absorption growths in the regions of 260–300 and 350–500 nm (although, on the tens of microseconds scale, slight increases occur, suggestive of a possible reaction of the alcohol radical with the platinum starting material). This quenching indicates that absorption growths in these areas have as their origin the reaction of OH. Furthermore, as the rates increase linearly with the concentration of $[PtCl_4]^{2-}$, the initial absorption spectra are associated with the nascent product(s) of the interaction of OH and $[PtCl_4]^{2-}$: the rationale for the shift of the peak at 455 nm in acidic media to 410 nm in highly alkaline solutions (Table I) will be discussed below. From the effects of varying the platinum complex concentration (85–507 μM) on the first stage of the absorption change, the value of the second-order rate constant for the reaction of OH and $[PtCl_4]^{2-}$ is calculated to be $(7 \pm 1) \times 10^9$ M^{-1} s^{-1} (11) for the following conditions: pH = 4.3–4.6, 10.0, 11.1; λ = 259, 299, 420–450 nm. This value is in good agreement with the rate constant reported by others for the reaction in neutral water.[3]

Several major new findings have arisen from our study of the OH reaction. In association with the initial growth in absorption, there is *no* corresponding change in conductivity in acidic media

Table II. Kinetic Summary for Interconversion of 450- to 410-nm Species and Associated Conductivity Change

			k(absorp)		*k*(conduct)	
originating reactants	[Pt], μM	pH	value, s^{-1}	λ, nm	value, s^{-1}	change
OH + $[PtCl_4]^{2-}$ [a]	85–507	3.4–4.6	$(1.4 \pm 0.3) \times 10^5$ [21] [b]	259–470	$(1.4 \pm 0.3) \times 10^5$ [8] [b]	increase
	250	9.0	1.2×10^5	471	1.0×10^5	decrease
	245	10.0	$(4 \pm 1) \times 10^4$ [3]	390–450		decrease[c]
	85, 250	11.1	$(1.2 \pm 0.2) \times 10^4$ [14]	349–471		decrease[c]
	288[d]	10.7	$(4.2 \pm 0.6) \times 10^4$ [10]	380–471		decrease[c]
e_{aq}^- + $[PtCl_6]^{2-}$ [e]	101–401	4.0–5.1	$(1.1 \pm 0.2) \times 10^5$ [22]	369–480	$(1.1 \pm 0.2) \times 10^5$ [6]	increase
H + $[PtCl_6]^{2-}$ [e]	98, 200	2.2, 2.6	$(1.5 \pm 0.2) \times 10^5$ [8]	410–470	$(1.3 \pm 0.2) \times 10^5$ [4]	increase
photochem of $[PtCl_6]^{2-}$ [f]	10–82	2.0–4.5	$(1.4 \pm 0.3) \times 10^5$ [30]	400–480	$(1.7 \pm 0.3) \times 10^5$ [15] [g]	increase

[a] Solutions saturated with N_2O. [b] 6-fold change in dose level had no effect on the values of the rate constants. [c] See text. [d] 1 mM NaOH solution aged for 22 h. [e] Solutions were saturated with argon and contained 0.11 M *tert*-butyl alcohol. One solution was done without alcohol for the e_{aq}^- case. [f] Wavelength of excitation 265 nm; for $[PtCl_6]^{2-}$ = 40 and 80 μM; no effect on laser intensity (6-fold) or addition of either 1 mM KCl or 150 μM $[PtCl_4]^{2-}$. [g] pH = 3.8–4.5 or 150 μM.

($\Delta\Lambda < |50|\ \Omega^{-1}\ cm^2$). This confirms experimentally Adams and co-workers' original proposal that the process involves OH addition, as no conductivity movement is expected:

$$OH + [PtCl_4]^{2-} \xrightarrow{+H_2O} [PtCl_4(OH)(H_2O)]^{2-} \qquad (6)$$

The absence of a conductivity change eliminates from further consideration an electron-transfer process because the hydroxide ion so generated (eq 7) would through its rapid reaction with

$$OH + [PtCl_4]^{2-} \rightarrow [PtCl_4]^- + OH^- \qquad (7)$$

proton lead in acidic media to a major decrease in conductivity, and this is not observed. In addition, the occurrence of $[PtCl_4]^-$ in a square-planar form here (or as a subsequent product) should be manifested according to the results of MS–Xα calculations by the presence of *two* intense CT transitions, one with a peak near 410 nm and the second at about 620 nm;[9] however, the latter is not found anywhere within the 500–720-nm region.

We have portrayed in eq 6 the platinum(III) product as being six-coordinate $[PtCl_4(OH)(H_2O)]^{2-}$ rather than five-coordinate $[PtCl_4(OH)]^{2-}$ for reasons based upon both experiment and theory. In the preceding paper, the calculated results obtained from the MS–Xα MO model predict that both square-pyramidal $[PtCl_4(OH)]^{2-}$ and tetragonally distorted $[PtCl_4(OH)(H_2O)]^{2-}$ will exhibit an intense CT peak near 450 nm; however, a critical difference arises in the 200–300-nm region.[11] For the five-coordinate species, no second intense CT band is expected above 200 nm; in contrast, a band with a maximum near 250 nm is anticipated for the six-coordinate case. Experimentally the initial absorption increase between 260 and 300 nm, which is associated with the OH reaction with $[PtCl_4]^{2-}$, is small (Figures 1 and 2); however, this is an artifact of the considerable absorption by $[PtCl_4]^{2-}$ in this region. If one corrects for the loss of starting material due to the OH reaction, then a rapid increase in absorption with decreasing wavelength is evident (solid circles in Figures 1 and 2). Attempts to locate a peak at wavelengths below 260 nm proved not to be feasible because, while there occurred substantial increases in absorption at 240 and 250 nm, major contributions from scattered light of longer wavelengths were now present; nevertheless, the steep absorption gradient (260–300 nm) argues in favor of a peak above 200 nm.

A second reason for favoring the designation $[PtCl_4(OH)(H_2O)]^{2-}$ is that its occurrence provides a reasonable framework to account for absorption and conductivity changes on progressing from acidic to basic media. The initial peak at 450 nm in acid (Figure 1) has shifted by pH 11.1 to 410 nm (Figure 2) with relatively little alteration at wavelengths below 300 nm; this suggests that the energy gap between the CT band in the visible region and the second one presumed to be near 250 nm has decreased. This narrowing of the energy difference is qualitatively consistent with the theoretical predictions for the situation where $[PtCl_4(OH)(H_2O)]^{2-}$ undergoes reaction in basic media with the hydroxide ion to yield $[PtCl_4(OH)_2]^{3-}$ as in eq 8.[11,27] Concomitantly, one expects a decrease in conductivity

$$[PtCl_4(OH)(H_2O)]^{2-} + OH^- \rightarrow [PtCl_4(OH)_2]^{3-} + H_2O \qquad (8)$$

owing to the consumption of OH^-, and this is observed experimentally. At pH 9, the rate of conductivity decrease is somewhat slower than the initial growth in absorption due to the reaction of OH and $[PtCl_4]^{2-}$ (eq 6), but by pH 10–11, the two rates are nearly the same and the conductivity level reaches its maximum value of $-200\ \Omega^{-1}\ cm^2$. This and the apparent shift of the peak to 410 from 450 nm in acidic media imply that, at high pHs, the rate of the hydroxyl radical reaction with $[PtCl_4]^{2-}$ (eq 6) is rate limiting with that of eq 8 being faster.

Subsequent to these initial developments, there transpire further changes in absorption (Figures 1 and 2). In alkaline media, the peak at 410 nm undergoes additional growth, but with essentially no associated change in conductivity. In acidic solutions, the decay in the band with a maximum near 450 nm occurs simultaneously with the growth of a new band having a peak at 415 nm (Table I). These developments are now accompanied by a conductivity increase, and the value of $+400 \pm 10\ \Omega^{-1}\ cm^2$ (7) is indicative of the release of 1 equiv of proton. As shown in Table II, the associated first-order rate constants for the conductivity and absorption movements are the same, and the value for the absorption phenomenon is in close agreement with reported measurements.[2,3] The intramolecular transformation originally proposed by Adams and co-workers to explain the interconversion of the 450-nm species to that at 410 nm is not in accord with this observed increase in conductivity.[2]

Critical to the interpretation of the aforementioned results is knowledge of the overall electrostatic charge on the 410-nm product in order to provide insight into its composition. Consistent with its designation as a Pt(III) species is our observation that it reacts on millisecond time scales with the mild reducing agent $[Fe(CN)_6]^{4-}$ to yield $[Fe(CN)_6]^{3-}$ and presumably a platinum(IV) product, although the latter was not observed optically.[28,29] At the concentrations of ferrocyanide used (25 and 50 μM), its presence did not affect the formation of $[PtCl_4(OH)(H_2O)]^{2-}$ or its subsequent transformation to the 410-nm intermediate; however, the latter's rate of reaction with $[Fe(CN)_6]^{4-}$ was sufficiently fast so as to obviate interference arising from the long-term decay of the 410-nm species (see below).

The rate of reaction of this Pt(III) complex and $[Fe(CN)_6]^{4-}$ increased as the ionic strength of the media was raised through the addition of $NaClO_4$, and the plot of the observed pseudo-first-order rate constant against the square root of ionic strength (μ) is shown in Figure 3a. The intercept leads to a value of the second-order rate constant for the ferrocyanide reaction of $(8.2 \pm 0.3) \times 10^5\ M^{-1}\ s^{-1}$ ($\mu \rightarrow 0$). The slope, which closely ap-

(27) While the energy difference should be smaller for $[PtCl_4(OH)_2]^{3-}$ than that for $[PtCl_4(OH)(H_2O)]^{2-}$, our expectation was for the former complex that the higher energy transition should have shifted to the red relative to that of the monohydroxy complex whereas experimentally it is the blue shift of the lower energy transition that appears to give rise to the narrowing of the energy gap.

(28) The reaction of the 410-nm species and $[Fe(CN)_6]^{4-}$ was studied at pH 5.8–6.0 (natural pH) to ensure that the ferrocyanide ion was not monoprotonated: the pK_a value of $[HFe(CN)_6]^{3-}$ is 4.2.[29]

(29) Chadwick, B. M.; Sharpe, A. G. *Adv. Inorg. Chem. Radiochem.* **1966**, *8*, 83–176.

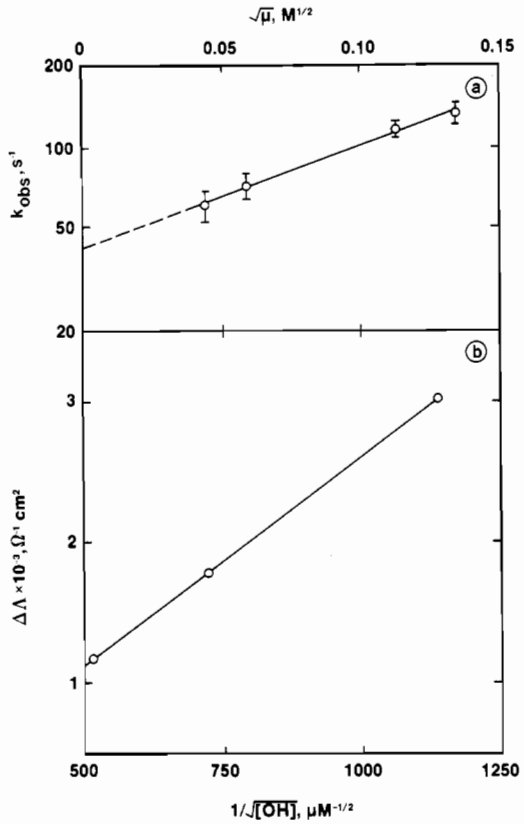

Figure 3. (a) Semilogarithmic plot of the observed rate constant for the reaction of the 410-nm Pt species and ferrocyanide versus the square root of the ionic strength of the N_2O-saturated solution at pH 6.0: 500 μM $[PtCl_4]^{2-}$, 50 μM $[Fe(CN)_6]^{4-}$, ionic strength adjusted with $NaClO_4$. Least-squares regression analysis: fit 0.995, intercept 41 ± 2 s^{-1}, slope 3.8 ± 0.2. (b) Plot of the change in the long-term conductivity ($\Delta\Lambda$) versus the reciprocal of the square root of the maximum micromolar concentration of the hydroxyl radical for N_2O-saturated solution containing 506 μM $[PtCl_4]^{2-}$ and 201 μM $[PtCl_6]^{2-}$ at pH 4.6. Least-squares regression analysis: fit 0.9998, intercept 320 ± 40 Ω^{-1} cm^2, slope 2.9 ± 0.4 Ω^{-1} cm^2 $\mu M^{1/2}$.

proximates the product of the two reactants' charges, is 3.8 ± 0.2; thus, it shows the 410-nm intermediate to carry an overall charge of −1. This finding serves to eliminate from consideration five-coordinate $[PtCl_4O]^{3-}$ and $[PtCl_3(OH)_2]^{2-}$, whose formation from $[PtCl_4(OH)(H_2O)]^{2-}$ would otherwise also be consistent with the observed increase in conductivity. The equivalent release of one proton from the first-order decay of the 450-nm species $[PtCl_4(OH)(H_2O)]^{2-}$ (Table II) coupled with a −1 charge on the resulting 410-nm species provides strong evidence that the interconversion process with an observed isosbestic point in acidic media at 440 nm is that of eq 9. Corroboration for the Pt(III) product

$$[PtCl_4(OH)(H_2O)]^{2-} \rightarrow [PtCl_2(OH)_2]^- + H^+ + 2Cl^- \quad (9)$$

being of a square-planar type is found in the results from theoretical calculations that indicate either *cis*- or *trans*-$[PtCl_2(OH)_2]^-$ will exhibit the requisite CT band with a peak near 410–415 nm.[11]

The interpretation of the situation in basic solution appears less straightforward: the interconversion rate decreases with increasing pH (Table II), and the overall conductivity movement of −200 Ω^{-1} cm^2 is somewhat greater than that of −120 Ω^{-1} cm^2 expected for the sequence of eq 8 followed by eq 10 (with the latter's rate

$$[PtCl_4(OH)_2]^{3-} \rightarrow [PtCl_2(OH)_2]^- + 2Cl^- \quad (10)$$

constant being smaller than that of eq 9).[30] The higher than expected value suggests that the decay of the dihydroxo reactant may involve not only eq 10 but also further consumption of hydroxide ion in a process such as that of eq 11, having in conjunction

$$[PtCl_4(OH)_2]^{3-} + OH^- \rightarrow [PtCl(OH)_3]^- + 3Cl^- \quad (11)$$

with eq 8 a predicted overall value of −240 Ω^{-1} cm^2. The fact that the absorption features of the 410-nm band in acidic and basic solutions are very similar (Table I) is consistent with the formation of several closely related products in basic media: this finds support in the similarity of the theoretically predicted spectra for the series of species $[Pt^{III}Cl_{4-n}(OH)_n]^-$ (n = 1–4)[11] and from the observation that the spectrum arising on irradiation of an aquated solution of $[PtCl_4]^{2-}$ (one aged for 22 h, Table I)[24] is not too different from that of a freshly prepared solution even though the rate constants for their formation differ to a greater extent (Table II).

The kinetics describing the long-term decay of the visible absorption band (0.01–0.2-s time scales) is complex, as has been noted also in previous studies,[2,3] and this is accompanied by conductivity movements, indicating further generation of proton. Changes neither in pH nor in the $[PtCl_4]^{2-}$ concentration (2-fold) noticeably alter the situation. However, the conductivity value increases with decreasing dose: in acidic media at low dose, the value approaches +300 Ω^{-1} cm^2 (overall movement of +700 Ω^{-1} cm^2). In contrast, the addition of 200 μM $[PtCl_6]^{2-}$ at pH 4.6, conditions under which e_{aq}^- continues to be scavenged by N_2O with no apparent effect on the formation of $[PtCl_2(OH)_2]^-$, does dramatically increase the conductivity value. At low dose, this amounts to about +3000 Ω^{-1} cm^2, which in photochemical terms is equivalent to encountering a quantum yield substantially in excess of unity such as observed in the steady-state photoaquation of $[PtCl_6]^{2-}$.[15] The functional form of the long-term change in conductivity obeys an inverse square-root dependence upon dose ([OH]) as shown in Figure 3b. While the kinetic complexities of the situation do not allow a detailed interpretation, this form is qualitatively consistent with Pt(III) entities catalyzing the aquation of $[PtCl_6]^{2-}$ in competition with their bimolecular decay. This result now provides direct support for the earlier proposals, based upon steady-state results, for such species acting as catalytic agents.[14,15]

Reaction of the *tert*-Butyl Alcohol Radical with $[PtCl_6]^{2-}$. Results from a survey of pulse-irradiated solutions of 400 μM $[PtCl_6]^{2-}$ (pH 4.5, saturated with N_2O or Ar) indicated that reactions of OH would complicate the desired studies of the reactions of e_{aq}^- and the H atom with the platinum(IV) complex. To minimize these potential complications, the scavenging of the OH radical by *tert*-butyl alcohol was studied in the presence of $[PtCl_6]^{2-}$. The choice of this particular alcohol was based upon the fact that it exhibits very low reactivity toward e_{aq}^- and the H atom.[8,21,25] In addition, the resulting β-hydroxy radical (eq 4) has proven to be unreactive on pulse radiolysis time scales toward a platinum(IV) dichloroamine complex ion, whereas this material and also $[PtCl_6]^{2-}$ show substantial levels of reactivity toward α-hydroxy radicals, for example the methanol radical.[2,5] The experiments were performed under the following conditions: pH 4.3, N_2O-saturated solutions containing 201 μM $[PtCl_6]^{2-}$ with 0.11 M alcohol or 623 μM platinum complex plus 0.51 M alcohol. For these situations, both e_{aq}^- and OH will be rapidly converted via eq 3 and 4 into the *tert*-butyl alcohol radical, and thus, near the end of the irradiation pulse, approximately 90% of the radicals will be the β-hydroxy species with a minor amount being the unscavenged H atom.

Under these conditions, a slow increase in absorption occurred in the visible region where the alcohol radical does not absorb,[26] and the resulting spectrum closely matches that for $[PtCl_2(OH)_2]^-$ (Table I). Concomitantly a conductivity increase transpired, and at low dose, the maximum value attained was +700 Ω^{-1} cm^2. The observed first-order rate constants for both phenomena proved to be first-order with respect to the concentration of $[PtCl_6]^{2-}$; however, their values increased slightly with a 3-fold increase in dose, indicating that in addition to its reaction with the platinum complex, the β-hydroxy alcohol radical was also exhibiting self-reaction.[26] From the effects of varying dose and Pt concentration,

(30) The possibility that eq 8 approaches a reversible-equilibrium situation has been considered, and while the kinetic data support this in a qualitative fashion, the calculated pK_a for $[PtCl_4(OH)(H_2O)]^{2-}$ of 10 is too high to account for the conductivity changes that would indicate a pK_a of ca. 9.

Table III. Kinetic Summary of Formation of 450-nm Species and Associated Conductivity Change

			k(absorp)		*k*(conduct)	
originating reactants	[Pt], μM	pH	value, s^{-1}	λ, nm	value, s^{-1}	change
$e_{aq}^- + [PtCl_6]^{2-}$ [a]	101, 380	4.4, 5.1	$(4.8 \pm 0.6) \times 10^5$ [9]	279–309, 435–450[b]	4.2×10^5 [2][c]	increase
$H + [PtCl_6]^{2-}$ [d]	98, 200	2.6	$(5 \pm 1) \times 10^5$ [5]	450[e]		*f*
photochem of $[PtCl_6]^{2-}$	40	3.0–4.4	$(4.8 \pm 0.5) \times 10^5$ [5]	435[e]		*f*

[a] Solutions contained 0.11 or 0.51 M *tert*-butyl alcohol; one experiment was also done without alcohol being present. [b] Decay in absorption (279–309 nm); growth at longer wavelengths. [c] [Pt] = 380 μM, pH 4.4. [d] Solutions were saturated with argon and contained 0.11 M *tert*-butyl alcohol. [e] Apparent isosbestic point. [f] See text.

the values of the second-order rate constants for the reaction of the complex ion are calculated to be $(6.1 \pm 0.8) \times 10^7$ M^{-1} s^{-1} (12) for the optical growth (370–460 nm) and for the conductivity increase $(6.0 \pm 0.5) \times 10^7$ M^{-1} s^{-1} (4). No intervening transients or processes such as that of eq 9 were observed, nor would they be expected given the slow rate of interaction between the platinum(IV) complex and the alcohol radical. The overall reaction is proposed to be that of eq 12, having an anticipated conductivity

$$[PtCl_6]^{2-} + {}^{\bullet}CH_2(CH_3)_2COH \rightarrow [PtCl_2(OH)_2]^- + 3Cl^- + 2H^+ + ClCH_2(CH_3)_2COH \quad (12)$$

change of ca. +860 Ω^{-1} cm^2: this value being slightly larger than that observed again implies the competitive presence of the self-reaction for the decay of the alcohol radical. The process of eq 12 is suggested to involve chlorine abstraction rather than a process leading to the oxidation of the β-hydroxy radical for the following reasons. The *tert*-butyl alcohol radical is a poor reducing agent, and if it were to be oxidized, the resulting conductivity increase would likely be substantially greater than that predicted for eq 12.[31] Furthermore, the reaction of the *tert*-butyl alcohol radical with $[IrCl_6]^{2-}$ has been shown to proceed by chlorine atom transfer, in analogy to that of eq 12.[32] With regard to the use of *tert*-butyl alcohol in the studies described below, the foregoing results indicate that while the occurrence of the alcohol radical reaction with $[PtCl_6]^{2-}$ precludes investigating long-term processes, it is not a significant interference with the studies of the shorter term processes of interest here.

Reactions Associated with e_{aq}^- and $[PtCl_6]^{2-}$. Studies on the reaction of the hydrated electron and the platinum(IV) chloro complex and on the subsequent reactions of the resulting platinum(III) transient species have been carried out in argon-saturated solutions at pH 4.4–5.1 containing 101–401 μM $[PtCl_6]^{2-}$ and generally 0.11 or 0.51 M *tert*-butyl alcohol. The latter has been used as described above to scavenge the hydroxyl radical, and the rate of interaction of the corresponding alcohol radical with $[PtCl_6]^{2-}$ (eq 12) is under our conditions sufficiently slow that this process does not contribute significantly to the observed absorption and conductivity changes within about the first 50 μs from the end of the irradiation pulse. During this period, three stages of alteration to the solution's conductivity can be identified and at least this number of changes to the absorption phenomenon also occur. Saturation of the solutions with nitrous oxide to scavenge e_{aq}^- (eq 3 followed by eq 4) eliminates these stages for both absorption and conductivity—this demonstrates that these events are associated with the reaction of e_{aq}^- and $[PtCl_6]^{2-}$.

Almost in coincidence with the end of the electron pulse is the presence of a conductivity level of about +400 Ω^{-1} cm^2 (relative to that of the media before irradiation), and this change is commensurate with that expected due to the generation of proton via solvent decomposition (eq 1). Closely associated in time is the rapid decay of the absorption (600–720 nm) due to the hydrated electron, and the corresponding rate has proven to be first order with respect to the concentration of $[PtCl_6]^{2-}$. The value of the second-order rate constant calculated from the data for the process of eq 13 is $(2.4 \pm 0.4) \times 10^{10}$ M^{-1} s^{-1} (3), and this number is in

$$[PtCl_6]^{2-} + e_{aq}^- \rightarrow [PtCl_6]^{3-} \quad (13)$$

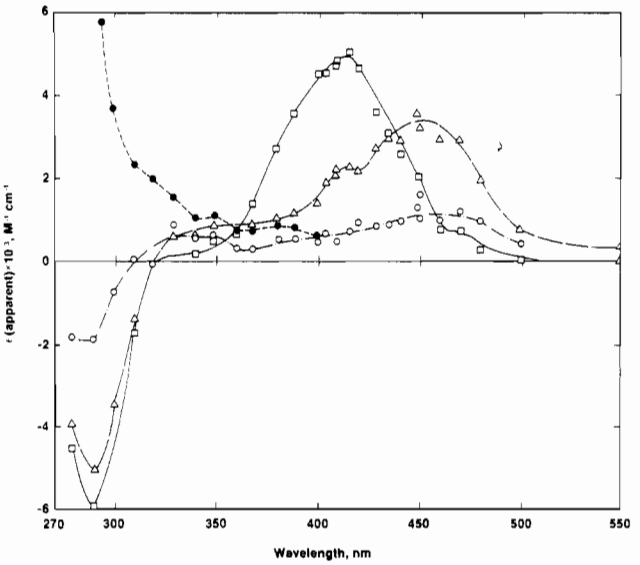

Figure 4. Absorption spectra of the products from the reaction of e_{aq}^- and $[PtCl_6]^{2-}$ (101 μM $[PtCl_6]^{2-}$, 0.11 M *tert*-butyl alcohol, Ar saturated, pH 5.1): (○) after 2 μs; (●) after 2 μs corrected for absorption loss of starting material, (△) after 5 μs; (□) after 35 μs.

good agreement with previously reported values for this reaction.[8] At lower wavelengths (280–320 nm) where the platinum(IV) complex absorbs appreciably, the absorption is observed also to decay rapidly. If one corrects for the loss of the starting material's absorption in this region, then the presence of an intensely absorbing band is apparent as depicted in Figure 4 (solid circles), whereas at wavelengths above 350 nm, very little absorption change is encountered at this early stage. Findings obtained from both experiment and theory indicate that $[PtCl_6]^{3-}$ exhibits an intense maximum near 260 nm.[5,10] There is also some expectation that other platinum(III) products such as $[PtCl_5(H_2O)]^{2-}$ and $[PtCl_4(H_2O)_2]^-$, potentially formed by rapid aquation of $[PtCl_6]^{3-}$, may also absorb significantly in this lower wavelength region so the possibility exists that absorption here may be indicative of more than one species.

The second identifiable stage is characterized by a further decrease in absorption in the range 280–320 nm and a concomitant growth of a band with a peak at 450 nm (Figure 4). Both of these movements obey a first-order rate law; the associated rate constants have the same value, and the changes are independent of platinum(IV) concentration (Table III). In the same manner, the conductivity undergoes a further increase of ca. +400 Ω^{-1} cm^2, and this also corresponds to the maximum development of the 450-nm band (Figure 4, spectrum at 5 μs). This feature in conjunction with the spectral similarity of the transient to that of $[PtCl_4(OH)(H_2O)]^{2-}$ (Table I), formed in the reaction of the hydroxyl radical with $[PtCl_4]^{2-}$ (eq 6), indicates that the monohydroxo complex is also being observed in the present circumstance.

This conclusion is reinforced by the fact that the third stage of reaction found here essentially mimics that encountered previously in the context of OH reacting with $[PtCl_4]^{2-}$: the spectral features for the resulting band with a peak at 415 nm, the values of the first-order rate constants describing the interconversion process (eq 9), and the accompanying increases in conductivity are the same within experimental error for these two situations

(31) Lilie, J.; Beck, G.; Henglein, A. *Ber. Bunsen-Ges. Phys. Chem.* **1971**, *75*, 458–465.
(32) Steenken, S.; Neta, P. *J. Am. Chem. Soc.* **1982**, *104*, 1244–1248.

(Tables I and II). In the present case, the overall conductivity change at the end of the third phase of reaction (ca. 35 μs) is about +1250 Ω^{-1} cm^2 after an allowance of 18% is made for the background contribution from the slow reaction of the *tert*-butyl alcohol radical with the platinum(IV) starting material (eq 12).[33] The experimental conductivity value is in accord with that of +1280 Ω^{-1} cm^2 predicted for the overall process shown in eq 14 plus the

$$[PtCl_6]^{3-} \rightarrow [PtCl_2(OH)_2]^- + 2H^+ + 4Cl^- \quad (14)$$

inclusion of 1 equiv of proton generated initially through the decomposition of water by irradiation (eq 1). Mechanistically, the three stages of reaction embodied in eq 14 can be accommodated within the framework of the electron attachment to $[PtCl_6]^{2-}$ (eq 13) being followed sequentially by eq 15, 16, and 9, with eq 9 yielding $[PtCl_2(OH)_2]^-$. The second and third phases

$$[PtCl_6]^{3-} \xrightarrow{2H_2O} [PtCl_4(H_2O)_2]^- + 2Cl^- \quad (15)$$

$$[PtCl_4(H_2O)_2]^- \rightarrow [PtCl_4(OH)(H_2O)]^{2-} + H^+ \quad (16)$$

of reaction are represented by eq 16 and 9 with the products of these processes being associated with the absorption bands with peaks at 450 and 415 nm, respectively. Because $[PtCl_6]^{3-}$ appears to exist even on the microsecond time scale at only very high concentrations of chloride and proton,[5] we propose that the first stage encompasses a sequence of rapidly occurring events beginning with the formation of this complex ion (eq 13) and leading to its subsequent aquation (eq 15): here we have shown for simplicity one possible product, $[PtCl_4(H_2O)_2]^-$. However, other closely related aquo species may be present and may contribute to the formation of the monohydroxo complex (eq 16). There is in addition some evidence that, at lower pHs, the deprotonation reaction of eq 16 may be reversible (see below).

Reactions Associated with the H Atom and $[PtCl_6]^{2-}$. Investigations into the reaction of the hydrogen atom and the hexachloroplatinum(IV) ion have been carried out under conditions (pH 2.2–2.7, Ar-saturated media) where the hydrated electron reacts rapidly with the proton (nanosecond scale) to form the H atom. A study of the interaction of the hydrogen atom with the *trans*-dichlorobis(ethylenediamine)platinum(IV) ion has shown by optical detection that a fast reaction occurs ($k = 4 \times 10^9$ M^{-1} s^{-1}) to yield by putative chlorine abstraction a platinum(III) species.[5] By analogy, one expects the primary reaction of $[PtCl_6]^{2-}$ to be that of eq 17 with the resulting products giving rise to a

$$H + [PtCl_6]^{2-} \xrightarrow{+H_2O} [PtCl_5(H_2O)]^{2-} + H^+ + Cl^- \quad (17)$$

substantial increase in conductivity. The probable platinum(III) product $[PtCl_5(H_2O)]^{2-}$ is conceivably an intermediate in the decay scheme for $[PtCl_6]^{3-}$ (eq 15), and thus the study of the hydrogen atom process affords potentially an alternative route to form platinum(III) species and ones likely to be germane to the electron case. At the same time, it offers the opportunity to investigate the effects of using pHs lower than those feasible in the hydrated electron reaction. In general, these expectations have been realized by working under conditions where *tert*-butyl alcohol (0.11 M) has been employed to scavenge the OH radical and the concentration of $[PtCl_6]^{2-}$ has been restricted to 97–200 μM to ensure that the electron reaction with proton prevails over its reaction with the platinum complex and that the latter's reaction with the *tert*-butyl alcohol radical is of minor influence.

On irradiation of such solutions, at least two stages for increase in conductivity and for changes in the visible absorption region (Figure 5) are encountered. Saturation of the media with oxygen, a facile scavenger of the hydrogen atom to give the perhydroxy radical, HO_2 (eq 5), which does not absorb appreciably above 300 nm, reduces the absorption and conductivity changes to less than about 20% of their values in the absence of O_2.[34,35] In deoxygenated solutions, the initial and rapid conductivity increase yields a change of ca. +400 Ω^{-1} cm^2, a value consistent with that expected for a chlorine-abstraction process (eq 17). While this and the accompanying absorption growth near 450 nm are not well-resolved from subsequent changes, the results lead to an estimate of 7×10^9 M^{-1} s^{-1} for the associated rate constant. A further stage of absorption increase occurs rapidly thereafter, giving rise to the spectrum shown in Figure 5 at 4 μs, and the rate law is first order and independent of platinum(IV) concentration (Table III). (It is unclear if this stage has a concurrent conductivity movement because the latter is continually increasing both before and after this event.) At pH 2.6, the resulting band with a peak at 455 nm exhibits features very similar to those observed in the reactions of OH with $[PtCl_4]^{2-}$ and of the electron with $[PtCl_6]^{2-}$ (Table I). However, at pH 2.2, the peak has shifted to about 445 nm and the apparent absorption coefficient is approximately half the value found at higher pHs—this implies that the process given in eq 16 may be reversible, and the predominate species may now be $[PtCl_4(H_2O)_2]^-$.

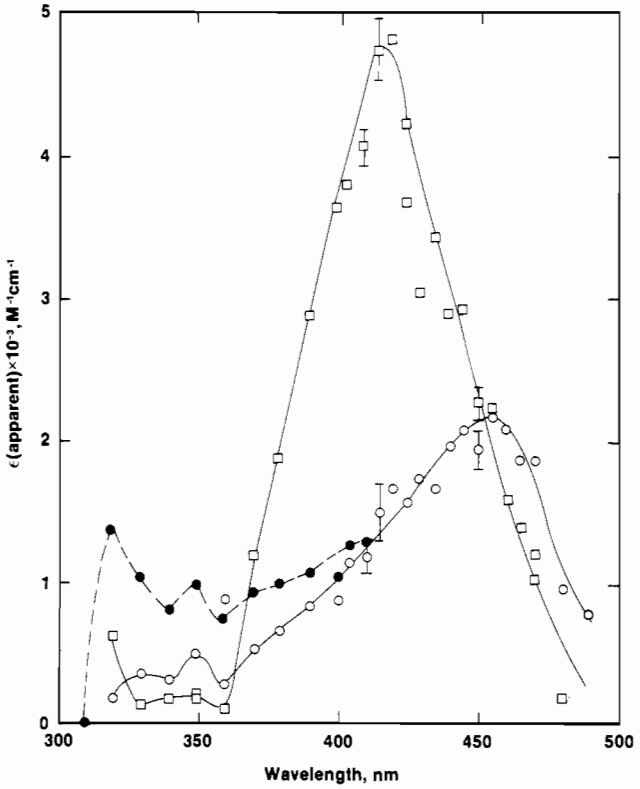

Figure 5. Absorption spectra of the products from the reaction of the H atom and $[PtCl_6]^{2-}$ (100 μM $[PtCl_6]^{2-}$, 0.11 M *tert*-butyl alcohol, Ar saturated, pH 2.6): (○) after 4 μs; (●) after 4 μs corrected for absorption loss of starting material; (□) after 35 μs.

As illustrated in Figure 5, the subsequent phase is characterized by a decay of the 455-nm band in association with the development of a new band with a maximum at 420 nm. These features and the accompanying increase in conductivity obey a first-order rate law, and the values of the rate constants are the same within experimental error and independent of pH and $[PtCl_6]^{2-}$ concentration (Table II). Although these kinetic and spectral attributes are very close to those for $[PtCl_2(OH)_2]^-$, its formation by an overall process such as that of eq 18 will be accompanied

$$H + [PtCl_6]^{2-} + 2H_2O \rightarrow [PtCl_2(OH)_2]^- + 3H^+ + 4Cl^- \quad (18)$$

by an increase of +1300 Ω^{-1} cm^2. This value is much too large

(33) The correction factor cited has been determined from measurements made on the corresponding N_2O-saturated solutions, where only the reaction of the *tert*-butyl alcohol radical and $[PtCl_6]^{2-}$ occurs.

(34) Hug, G. L. *Natl. Stand. Ref. Data Ser. (U.S., Natl. Bur. Stand.)* **1981**, *NSRDS-NBS69*.

(35) While, in oxygenated solutions, the reactions of O_2 with e_{aq}^- and with the *tert*-butyl alcohol radical will occur to some extent, these are not expected to be complicating factors: the resulting O_2^- will be protonated to give HO_2, and the peroxy form of the alcohol radical does not absorb above 350 nm.[26,34]

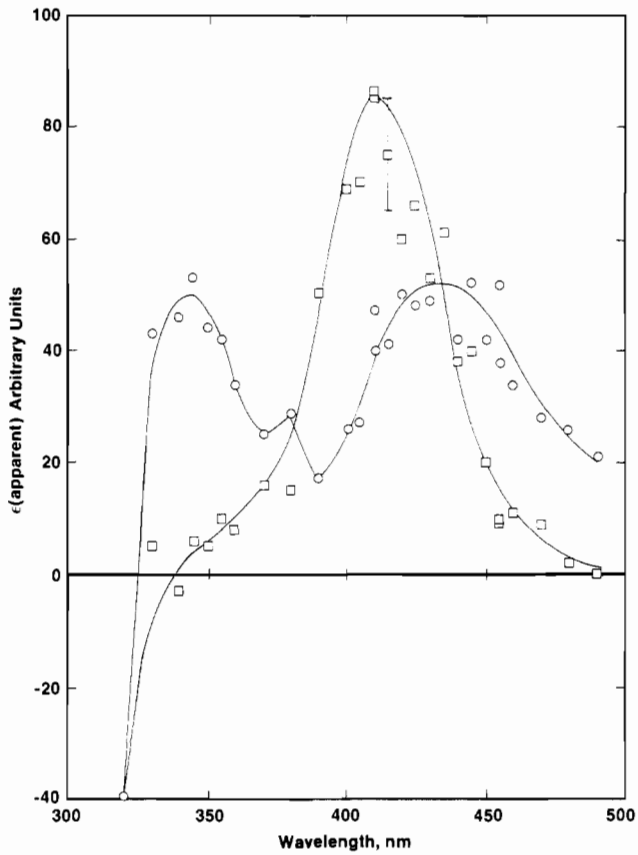

Figure 6. Absorption spectra of the products arising from the 265-nm photolysis of 40 μM $[PtCl_6]^{2-}$ at pH 4.5: (○) after 3 μs; (□) after 45 μs.

to accommodate the observed value of $+1020 \pm 40\ \Omega^{-1}\ cm^2$ (3). After allowance is made for a background contribution (18%) from the reaction of the *tert*-butyl alcohol radical (eq 12), two overall reactions, each with a change of ca. $+850\ \Omega^{-1}\ cm^2$, as given in eq 19 and 20 are possible candidates. On theoretical grounds,

$$H + [PtCl_6]^{2-} + 2H_2O \rightarrow [PtCl_2(OH)(H_2O)] + 2H^+ + 4Cl^- \quad (19)$$

$$H + [PtCl_6]^{2-} + H_2O \rightarrow [PtCl_3(OH)]^- + H^+ + 3Cl^- \quad (20)$$

the platinum(III) products are predicted to have close spectral similarities to each other and to $[PtCl_2(OH)_2]^-$.[11] Given this circumstance, a choice between these possibilities is not feasible although intermediate steps involving species such as $[PtCl_4(H_2O)_2]^-$ seem probable. To further aid in the elucidation of the possible mechanistic features, investigations into the laser-flash photolysis of $[PtCl_6]^{2-}$ have been carried forth as described below.

Laser Photolysis of $[PtCl_6]^{2-}$ at 265 nm. The photolytic studies have been carried out on argon-saturated solutions containing 8–82 μM of complex between pHs 2.0 and 4.5. The wavelength of 265 nm corresponds to irradiation of the peak of an intense ligand-to-metal CT band,[36] and previous investigations performed in this spectral region have established the occurrence of both photoredox and photoaquation modes.[4,15] The latter mode is the predominant one, and this leads to the formation of $[PtCl_5(H_2O)]^-$ as in eq 21.

$$[PtCl_6]^{2-} + H_2O \xrightarrow{h\nu} [PtCl_5(H_2O)]^- + Cl^- \quad (21)$$

In the region of ca. 240–300 nm, the aquo product absorbs less than does the starting material, and this aspect accounts in large measure for the significant decreases in absorption on irradiation as portrayed in Figure 6 at the lower wavelengths. The reverse situation exists between 220 and 240 nm, and this provides a window within which one can observe the formation of the aquo product. Conductivity detection offers a complementary view because the monoaquo species exhibits a deprotonation reaction (eq 22) with a pK_a value of 3.8.[37] Cox and co-workers have

$$[PtCl_5(H_2O)]^- \rightleftharpoons [PtCl_5(OH)]^{2-} + H^+ \quad (22)$$

reported for steady-state photolysis that the quantum yield for aquation is less than 0.1 (270 nm) in the presence of Cl_2, but in the absence of this oxidizing agent, the yields are now substantially in excess of 1.[15] This contrasting behavior provides strong circumstantial evidence that Pt(III) species can thermally catalyze the aquation of the platinum(IV) complex ion. The formation of the platinum(III) species appears to occur via a photoredox process, which is a minor process relative to that of aquation: Wright and Laurence in their conventional flash photolysis study indicate the ratio of photoaquation to photogeneration of Pt(III) to be about 10:1.[4] Photoredox is signified by the presence at 50 ms of the characteristic Pt(III) band with a peak at 410 nm, but in this earlier work, no evidence was found for a preceding band at 450 nm.

Recent results obtained from chlorine atom scavenger experiments and from picosecond absorption measurements have shown that the nascent photoredox act is one of Pt–Cl homolytic bond cleavage.[5,7,38] The platinum(III) product of eq 23 exhibits two

$$[PtCl_6]^{2-} + h\nu \rightarrow [PtCl_5]^{2-} + Cl \quad (23)$$

intense CT peaks at 440 and 640 nm, and these features in conjunction with results from MS–Xα calculations indicate the product to be a square-pyramidal form of $[PtCl_5]^{2-}$.[7] This species decays very rapidly by first-order kinetics with a lifetime of 210 ± 10 ps. In the present study, the duration of our laser pulse was about 20 ns, and thus while a direct link between this transient and those observed here is not clearly established, it seems highly probable that the ones discussed below do represent products derived from the decay of the short-lived $[PtCl_5]^{2-}$.

Experimentally we observe within a period of about 40 μs from the end of the laser-flash absorption changes that can be divided into three regions on the basis of their different kinetic behaviors. In the 220–310-nm region, very rapid transformations (<1 μs) occur with little change thereafter to yield at pH 4.1 a maximum at 230 nm, a minimum at 275 nm, and a crossover point at 245 nm: these features correspond to those reported for aquation of $[PtCl_6]^{2-}$.[4,15] Between 400 and 480 nm, the platinum(III) species with a peak at 410 nm is found (Table I) in accord with earlier findings;[4] however, we now observe that this band is preceded by the formation and subsequent decay of a band at 445 nm (Figure 6). The intervening region (ca. 310–380 nm) appears to be an overlapping area between those dominated by the absorption of the aquation product(s) and of the platinum(III) species. In addition, absorption contributions near 340 nm at the initial stage seem to arise from the presence of chlorine atom, as there is a marked enhancement in absorption on addition of 1 mM KCl: the chlorine atom reacts rapidly with chloride ion to form Cl_2^- that absorbs more intensely than does the chlorine atom.[39,40] Outside of the interval of 310–380 nm, the presence of chloride ion has no noticeable effect on the absorption (or on the related kinetic phenomena).

For the conductivity, at least two stages of increase are encountered in acidic media. A very quick increase takes place on the submicrosecond scale, and this major component accounts at pH 4.5 for about 90% of the change occurring within the initial 40-μs period. The minor part correlates with the slower absorption transformations ascribed to the platinum(III) complexes (Table II).

(36) Goursot, A.; Penigault, E.; Chermette, H. *Chem. Phys. Lett.* **1983**, *97*, 215–220.
(37) Davidson, C. M.; Jamieson, R. F. *J. Chem. Soc., Faraday Trans. 1* **1965**, *61*, 2462–2467.
(38) Rehorek, D.; Dubose, C. M.; Janzen, G. *Inorg. Chim. Acta* **1984**, *83*, L7–L8.
(39) Jayson, G. G.; Parsons, B. J.; Swallow, A. J. *J. Chem. Soc., Faraday Trans. 1* **1973**, *69*, 1597–1607.
(40) Kläning, U. K.; Wolff, T. *Ber. Bunsen-Ges. Phys. Chem.* **1985**, *89*, 243–245.

The major alteration to the conductivity is attributable to the photoaquation on the basis of the following. The observed first-order rate constant k_{obs}, describing this initial stage of increase, depends linearly upon the proton concentration over the range pH 2.95–4.5: $k_{obs} = k_i + k_s[H^+]$ with $k_i = (1.1 \pm 0.2) \times 10^7\ s^{-1}$ and $k_s = (4.7 \pm 0.4) \times 10^{10}\ M^{-1}\ s^{-1}$ from a least-squares regression analysis (index of fit 0.934). With use of these values for the forward and reverse processes of the acid–base reaction for $[PtCl_5(H_2O)]^-$ (eq 22), the pK_a value is calculated to be 3.6 ± 0.2. A second estimate obtained from the variation of $\Delta\Lambda$ with pH gives 4.1 ± 0.2. While these two estimates diverge slightly, they are nevertheless close to the reported pK_a value of 3.8.[37] From the comparison of the initial conductivity with that found for photoelectron production from $[Fe(CN)_6]^{4-}$ (see Experimental Section), the quantum yield for photoaquation is on the order of 0.5, which is higher than that ($\phi < 0.1$) cited by others for steady-state photolysis.[15]

The formation of platinum(III) intermediates is signified by two stages of absorption change in the 400–480-nm region: there may also be an earlier phase associated with rapid decreases in the range 300–350 nm, but this could not be resolved from the subsequent events. As shown in Figure 6, a band with a peak near 445 nm occurs within 3 μs, and its development obeys a first-order rate law (Table III). Less clear is the possible occurrence of a concomitant conductivity increase because it is interspersed between the major initial change and a subsequent increase.

The latter event coincides with the decay of the 445-nm band and the accompanying growth of a new band with a peak at 410 nm (Table I). All of these movements exhibit first-order rate laws, and the rate constants are the same within experimental error and independent of the addition of 1 mM KCl or of 148 μM $[PtCl_4]^{2-}$ (Table II). The presence of the platinum(II) complex does, however, approximately double the absorbances of both the 445- and 410-nm bands and also the conductivity level associated with the interconversion process. The clear implication is that chlorine atom generated in the photoredox process (eq 23) is now being scavenged by $[PtCl_4]^{2-}$ to yield further amounts of the platinum(III) materials.

To explain the fact that the presence of $[PtCl_4]^{2-}$ increases the yields by a factor of 2 without altering the other features, we propose that there is a point of commonality, namely the formation of $[PtCl_5(H_2O)]^{2-}$ via eq 24 and 25 with eq 25 being preceded

$$Cl + [PtCl_4]^{2-} + H_2O \rightarrow [PtCl_5(H_2O)]^{2-} \quad (24)$$

$$[PtCl_5]^{2-} + H_2O \rightarrow [PtCl_5(H_2O)]^{2-} \quad (25)$$

by eq 23. The occurrence of this intermediate also accounts for the nascent reaction of the H atom with $[PtCl_6]^{2-}$ (eq 17), and it is likely to occur via aquation of $[PtCl_6]^{3-}$ formed in the reaction of e_{aq}^- and $[PtCl_6]^{2-}$; the results from these cases suggest that $[PtCl_5(H_2O)]^{2-}$ quickly undergoes aquation to give $[PtCl_4(H_2O)_2]^-$. From this point on, the subsequent stages of behavior are well-defined. The strong spectral and kinetic correspondence between these features here at ca. pH 4 and those for the reaction of OH and $[PtCl_4]^{2-}$ under similar conditions indicates that essentially the same sequences are taking place, that is eq 16 followed by eq 9. Even though the conductivity change predicted by eq 16 is not clearly evident in this instance, it is significant to our proposal that as one progresses to a lower pH of 2.4, the absorbance at 450 nm is now about half that at pH 4.5 and the apparent isosbestic point has shifted from 435 nm (Table I) to about 450 nm. These trends are very reminiscent of the effects of low pH found in the H atom case, which we attribute to eq 16 being partly reversible under low-pH conditions. On the basis of the release of 2 equiv of proton (eq 16 and 9), the fact that these changes account for 11 ± 2% (3) of the conductivity increase by 40 μs at pH 4.5 and the estimated quantum yield for photoaquation, then an upper limit to the quantum yield for the photoredox process (eq 23) is 0.05.

Investigations into the photochemical behavior of $[PtCl_6]^{2-}$ on longer time scales revealed features at pH 4.0 very similar to those encountered in the case of the reaction of OH and $[PtCl_4]^{2-}$.

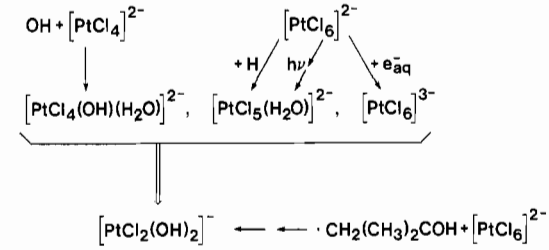

Figure 7. Overview of proposed reaction scheme.

Because the absorption signals were relatively low, it was not feasible experimentally to follow the full decay of the 410-nm band (time > 0.1 s). In contrast, the increase in conductance permitted observations to be made throughout the course of change, which lasted up to 10 s under our conditions. The associated rate law is complex; neither second-order nor first-order kinetic expressions adequately describe it. Both the rate and the level of the conductivity increase are not noticeably affected by changing the concentration of $[PtCl_6]^{2-}$ from 40 to 82 μM or upon adding 145 μM $[PtCl_4]^{2-}$; however, they are sensitive to dose, this being given here by the laser intensity. The functional form for the long-term increase in conductivity is found to be inversely dependent upon the square root of the dose over its change by 5-fold. This situation is analogous to that described above (Figure 3b) in the context of the reaction of the hydroxyl radical with $[PtCl_4]^{2-}$, and it provides an additional, direct line of support for platinum(III) species catalyzing the aquation of $[PtCl_6]^{2-}$.

Summary. Five different routes have been shown to lead to the formation of platinum(III) complex ions, and Figure 7 offers a schematic overview of the situation. The foregoing experimental results in combination with the findings derived from the theoretical calculations establish a consistent picture for the occurrence of two structural categories for the platinum(III) transients. Under our conditions, the shorter lived ones are of a six-coordinate, distorted-octahedral type, and these are exemplified in Figure 7 by the known or likely species formed as the primary reaction products. The interrelationships between these and related complexes involve aquation and acid–base processes. At longer time scales, these six-coordinate entities decay to yield four-coordinate platinum(III) ions that are describable within the general framework of square-planar structures: it is pertinent to note that, to our knowledge, the only monomeric platinum(III) compound isolated and well-characterized to date is of the square-planar type.[41] At moderate pHs (near 4), the main species encountered is that of $[PtCl_2(OH)_2]^-$. The results obtained by the MS–Xα method indicate that the cis and trans isomeric forms are expected to have very similar absorption spectra.[11] Consequently, the situations discussed here may involve the presence of one or both of these isomers, and in addition, the evidence points to the occurrence of related complexes at more acidic pHs or in basic media.

In the reaction of the hydroxyl radical and $[PtCl_4]^{2-}$, the mechanism leading from the primary to the secondary stages seems relatively well-defined, for example eq 6 followed by eq 9. In the reactions involving $[PtCl_6]^{2-}$, the sequences of events are considerably more complicated, and the possibility exists for the presence of a multiplicity of pathways at least in the earlier stages of reaction. Notwithstanding these potential complexities, the major features encountered with the platinum(III) aquo–chloro complex ions exhibit a close parallelism to those found for platinum(III) amine systems.[12,42]

Direct evidence has been presented here in both photolytic and radiolytic contexts for the longer lived platinum(III) species functioning as a catalytic agent(s) in the thermal aquation of $[PtCl_6]^{2-}$. The conditions of our work that have been dictated in part by the response characteristics of the conductivity apparatus are considerably different from those employed in studies per-

(41) Usón, R.; Forniés, J.; Tomás, M.; Menjón, B.; Sunkel, K.; Bau, R. *J. Chem. Soc., Chem. Commun.* **1984**, 751–752.
(42) O'Halloran, T. V.; Lippard, S. J. *Isr. J. Chem.* **1985**, *25*, 130–137.

taining to steady-state photoinduced aquation or ligand exchange where high concentrations of proton and chloride ion have been present.[14,15,43] Since the species $[PtCl_6]^{3-}$ has been observed to be relatively more stable at high HCl concentrations (conditions closer to the earlier photolysis experiments), the inference appears to be that this catalytic behavior is not restricted to a particular type of platinum(III) entity but is a more general feature, albeit the catalytic efficacy may vary considerably between different species.[5]

Acknowledgment. The financial support provided by the Natural Sciences and Engineering Research Council of Canada to W.L.W. and by the North Atlantic Treaty Organization (Project No. 0680/85) is very much appreciated.

Registry No. $[PtCl_4]^{2-}$, 13965-91-8; $[PtCl_6]^{2-}$, 16871-54-8; $^{\bullet}OH$, 3352-57-6; H, 12385-13-6; $^{\bullet}CH_2C(CH_3)_2OH$, 5723-74-0.

(43) Dreyer, R.; König, K.; Schmidt, H. *Z. Phys. Chem. (Leipzig)* **1964**, *227*, 257-271.

Contribution from the Inorganic Chemistry Laboratory, South Parks Road, Oxford OX1 3QR, U.K.

Polyhedral Skeletal Electron Pair Theory of Bare Clusters. 1. Small Silicon Clusters

Tom Slee, Lin Zhenyang, and D. M. P. Mingos*

Received November 11, 1988

The polyhedral skeletal electron pair theory, which has proved so successful in rationalizing the structures of ligated clusters, is applied to the structures of small clusters of silicon atoms formed in molecular beams. The PSEPT approach is able to account for many structural features of these small silicon clusters. A number of structures considered earlier as candidates for stable structures of a cluster of given nuclearity are shown to be ruled out by application of the PSEPT approach. Neutral silicon clusters have $2n$ electron pairs. The deltahedral geometries exhibited by boranes would be characterized for silicon atoms by $2n + 1$ electron pairs, and so these geometries are not stable. Small silicon clusters are shown to achieve a stable closed-shell electron configuration with a substantial HOMO–LUMO gap by two mechanisms: oblate distortion from the pseudospherical deltahedron to remove one axially antibonding orbital from the bonding region and capping of a suitable pseudospherical polyhedron. The PSEPT approach also suggests why silicon clusters of nuclearity 4, 6, 7, and 10 are more stable than those of nuclearity 5, 8, and 9.

Introduction

Ligated clusters have been actively investigated for more than 20 years, and their study can be reasonably described as a mature science. Synthetic procedures have been developed that have resulted in cluster compounds for the majority of transition-metal and main-group atoms, and their structures both in the solid state and in solution have been determined by using X-ray crystallographic and spectroscopic techniques.[1] Furthermore, their structures can be rationalized by using a set of simple electron-counting rules that relate the topology of the structure to the pattern of bonding and nonbonding molecular orbitals generated by a specific three-dimensional arrangement of atoms. This theory, described as the polyhedral skeletal electron pair theory,[2,3] has been underpinned by Stone's tensor surface harmonic theory.[4]

The study of clusters formed in molecular beam experiments or by matrix isolation techniques is a much more recent development.[5] Although the major thrust in this area has been directed toward naked metal clusters, there has also been considerable recent interest in clusters of main-group elements and particularly of semiconductors. The nature of the molecular beam experiments precludes direct structural studies by X-ray and electron diffraction techniques, but fortunately when the clusters are being formed from light atoms very accurate molecular orbital techniques can be used reliably to predict the cluster geometries and stabilities.[6] Such a study has been completed by Raghavachari and his coworkers on silicon clusters Si_n (n = 3–10)[7] following earlier work by other researchers using more approximate techniques.[8]

To date the degree of interaction between researchers in the ligated and beam cluster fields has been limited, and a major aim of this paper is to demonstrate the applicability of the ideas developed for ligated clusters from the polyhedral skeletal electron pair theory to naked silicon clusters formed in molecular beam experiments.

The central feature of the polyhedral skeletal electron pair theory is that particular classes of three-dimensional structures have characteristic closed-shell requirements. For example, deltahedral clusters are characterized by $4n + 2$ valence electrons, e.g., $B_nH_n^{2-}$ (n = 5–12),[3,9a] and three-connected clusters by $5n$ valence electrons, e.g., C_nH_n (n = even, 4–20).[9b] These closed-shell requirements maximize the element–element bonding interactions and create a favorable HOMO–LUMO gap. An important implication of this theory is that if the electron count is changed the structure will distort in such a way as to enlarge the HOMO–LUMO gap and by implication strengthen cluster bonding. For example, in the series $B_nH_n^{2-}$, $B_nH_n^{4-}$, and $B_nH_n^{6-}$ the closo-deltahedral cluster observed in the first structure is progressively opened up in the subsequent nido and arachno structures.[10]

In the silicon clusters, Si_n, there are always $4n$ valence electrons, which is two fewer than that required to satisfy the closed-shell requirements for closo deltahedra. Therefore, the principal question to be addressed is as follows: How can the deltahedral structures be distorted to create $2n$ bonding and nonbonding molecular orbitals and a sizeable HOMO–LUMO gap? The success of the polyhedral skeletal electron pair theory (PSEPT) for ligated clusters suggests strongly that such arrangements, if available, will be the most stable for Si_n clusters.

Skeletal Electrons in Silicon Clusters

Tensor surface harmonic (TSH) theory provides a theoretical framework for constructing qualitatively the molecular orbital manifold of pseudospherical clusters. For *closo*-boranes (other

(1) For a survey, see: Johnson, B. F. G. Ed. *Transition Metal Clusters*; Wiley: Chichester, England, 1980.
(2) (a) Mingos, D. M. P. *Nature Phys. Sci.* **1972**, *236*, 99. (b) Mingos, D. M. P. *Acc. Chem. Res.* **1984**, *17*, 311.
(3) (a) Wade, K. *Adv. Inorg. Chem. Radiochem.* **1976**, *18*, 1. (b) Wade, K. In *Transition Metal Clusters*; Johnson, B. F. G., Ed.; Wiley: Chichester, England, 1980.
(4) (a) Stone, A. J. *Inorg. Chem.* **1981**, *20*, 563. (b) Stone, A. J. *Mol. Phys.* **1980**, *41*, 1339. (c) Stone, A. J. *Polyhedron* **1984**, *3*, 1299.
(5) Several recent journal issues have been devoted to the subject. For example: (a) *Chem. Rev.* **1986**, *86*(3). (b) *Surf. Sci.* **1985**, *156*, Parts 1 and 2. (c) *Ber. Bunsen-Ges. Phys. Chem.* **1984**, *88*, 187–322. (d) *Adv. Chem. Phys.* **1987**, *70*, Parts 1 and 2.
(6) Koutecky, J.; Fantucci, P. *Chem. Rev.* **1986**, *86*, 539.
(7) (a) Raghavachari, K. *J. Chem. Phys.* **1985**, *83*, 3520. (b) Raghavachari, K. *J. Chem. Phys.* **1986**, *84*, 5672. (c) Raghavachari, K.; McMichael Rohlfing, C. *J. Chem. Phys.* **1988**, *89*, 2219.
(8) (a) Pacchioni, G.; Koutecky, J. *J. Chem. Phys.* **1986**, *84*, 3301. (b) Tomanek, D.; Schlüter, M. *Phys. Rev. Lett.* **1986**, *56*, 1055. (c) Tomanek, D.; Schlüter, M. *Phys. Rev. B* **1987**, *36*, 1208. (d) Ballone, P.; Andreoni, W.; Car, R.; Parinello, M. *Phys. Rev. Lett.* **1988**, *60*, 271.
(9) (a) Johnston, R. L.; Mingos, D. M. P. *J. Chem. Soc., Dalton Trans.* **1987**, 647. (b) Johnston, R. L.; Mingos, D. M. P. *J. Organomet. Chem.* **1985**, *280*, 407.
(10) Muetterties, E. L., Ed. *Boron Hydride Chemistry*; Academic Press: New York, 1975.

0020-1669/89/1328-2256$01.50/0